Magnetoelectric effect in multiferroic $NdMn_2O_5$*

Syed Hamad Bukhari† and Javed Ahmad

Department of Physics, Bahauddin Zakariya University, Multan 60800, Pakistan

(Received 30 July 2016; revised manuscript received 25 September 2016; published online 30 November 2016)

We have measured the dielectric constant for $NdMn_2O_5$ in an external magnetic field to map out the magnetoelectric phase diagram. The phase diagram corresponds well with the previously reported data of neutron diffraction and magnetic susceptibility. Our main finding is the observation of a dielectric anomaly in the low temperature phase with a strong magnetoelectric effect, which is attributed to the independent Nd^{3+} ordering. Moreover, the absence of the dielectric anomaly in the paramagnetic phase is discussed, keeping in view the exchange interaction and its dependence on the rare-earth R^{3+} ionic radius.

Keywords: sol–gel synthesis, dielectric constant, magnetoelectric effect, phase transition

PACS: 81.20.Fw, 78.20.Ci, 75.85.+t, 77.80.B– **DOI:** 10.1088/1674-1056/26/1/018103

1. Introduction

Magnetoelectric multiferroic compounds are a subject of significant consideration because they are characterized simultaneously by different magnetic and electric ferroic orders that are coupled. The magnetoelectric effect resulting from such strong coupling is stemming for exceptional materials, which opens a new horizon for the next generation applications in functional devices. In recent years, the magnetically frustrated multiferroic RMn_2O_5 family of oxides have attracted a great deal of attention due to the strong coupling between the magnetic and electric ferroic orders.[1,2] The magnetoelectric effect revealed in RMn_2O_5 is due to a variety of phenomena, among them are magnetically induced polarization (P) in $HoMn_2O_5$,[1] magnetically reduced P in $ErMn_2O_5$,[1] magnetically flipped P in $TbMn_2O_5$[2] and $GdMn_2O_5$,[3] and magnetically flopped P in $TmMn_2O_5$[4] and $YbMn_2O_5$,[5] all arising in the low temperature phase. A reversible magnetocaloric effect has also been observed in $HoMn_2O_5$.[6] Moreover, the magnetoelectric coupling effect has also been studied in thin films.[7–9]

The main structure of all manganese RMn_2O_5 compounds crystallizes in the isostructural orthorhombic symmetry with space group *Pbam*.[10,11] All members of RMn_2O_5 are characterized as the geometrically frustrated system because a slight deviation from their mean structure has been detected.[12] In a unit cell, there exist two manganese ions with different valances and positions: 4h for Mn^{3+} ($t_{2g}^3e_g^1$) forming $Mn^{3+}O_5$ square pyramids and 4f for Mn^{4+} ($t_{2g}^3e_g^0$) with corner sharing $Mn^{4+}O_6$ octahedra. These manganese ions together with oxygen coordination form a loop of five Mn ions, three Mn^{3+} and two Mn^{4+}. In each loop, there are three inequivalent magnetic superexchange interactions in the *ab* plane between the Mn^{3+} and Mn^{4+} ions, which are usually referred to as magnetic interactions J_3, J_4, and J_5. The J_3 and J_4 magnetic interactions correspond to the exchange interactions between the magnetic moments of Mn^{3+} and Mn^{4+}, and J_5 corresponds to the magnetic interaction between two Mn^{3+} magnetic moments. Considering the *ac* plane, one can easily outline two Mn^{4+}–Mn^{4+} magnetic interactions, namely, J_1 and J_2. The J_1 is responsible for the magnetic interaction between adjacent Mn^{4+} spins through oxygen at the R^{3+} layer and depends on the radius of the R^{3+} ion, which directly affects the z component (k_z) of the propagation vector (k).[13,14] Blake *et al.* have studied the crystal and magnetic structures of RMn_2O_5 (R = Tb, Ho, Dy) as a function of temperature by using neutron diffraction. They found that the spin arrangement of Mn ions is identical within the *ab* plane of the commensurate phase for each system. It was also suggested that a shift of the Mn^{3+} cations gives rise to a net polarization along the b axis due to the canted antiferroelectric structure.[15] Moreover, the radius of R^{3+} is essentially insensitive in the *ab* plane, while it determines the exchange interaction with adjacent Mn^{4+} spins in the *ac* plane.

The key issue in the family of RMn_2O_5 is to elucidate the influence of R^{3+} on the magnetoelectric properties and its effect on the Mn magnetic ordering through J_1. It is important to note that RMn_2O_5 compounds with large size R^{3+} (La and Pr) are not ferroelectrics.[16] Interestingly, compounds with small size R^{3+} (Nd to Yb) all present a similar behavior, with the largest polarization in the commensurate (CM) phase,[2] except in the case of $NdMn_2O_5$. Very recently, it was observed that the multiferroic $NdMn_2O_5$ exhibiting the largest polarization along the b axis in the incommensurate (ICM) phase[17] differs from other RMn_2O_5. This makes $NdMn_2O_5$ an interesting compound to study because it lies between the nonferroelectric $PrMn_2O_5$ and ferroelectric $SmMn_2O_5$ and possesses a different magnetic origin for the ferroelectric polarization.

A spin–phonon interaction has been observed in the para-

*Project supported by Higher Education Commission (HEC) of Pakistan through its IRSIP scholarship program (IRSIP 27 PS 28).

†Corresponding author. E-mail: bukhari.hamad@gmail.com

© 2017 Chinese Physical Society and IOP Publishing Ltd

magnetic phase of $R\mathrm{Mn_2O_5}$ (R = Eu, Dy, and Bi) with the detection of Raman phonons[18] and infrared active phonons in $\mathrm{DyMn_2O_5}$.[19] More interestingly, it was found that the phonon anomalies in the paramagnetic phase show a strong dependence on the R^{3+} ions.[18] Very recently, we observed an anomalous behavior in the dielectric constant slightly above the Néel temperature in $\mathrm{GdMn_2O_5}$[20] and $\mathrm{DyMn_2O_5}$.[21] In this regard, we are motivated to conduct temperature dependent dielectric measurements in the paramagnetic phase of $\mathrm{NdMn_2O_5}$ to reveal the existence of a dielectric response at high temperature in this compound. As Nd^{3+} has a larger ionic size as compared to Gd^{3+} and Dy^{3+}, so we expect some interesting results that can shed light on the role of the R^{3+} ion in the family of $R\mathrm{Mn_2O_5}$.

Here, we report on the dielectric properties of polycrystalline $\mathrm{NdMn_2O_5}$ in the temperature range T = 2–60 K with applied magnetic field H = 0–12 T. Based on our results, we provide a comprehensive explanation about the magnetoelectric transition in the $\mathrm{NdMn_2O_5}$ system and also construct the magnetoelectric phase diagram. In addition, we will emphasize on the role of the R^{3+} ion in the paramagnetic phase.

2. Experimental setup

A polycrystalline sample of $\mathrm{NdMn_2O_5}$ was prepared by using the sol–gel method.[20,22] X-ray diffraction (XRD) measurement was performed with a Rigaku powder x-ray diffractometer using Cu $K\alpha$ radiation in the 2θ range from 20° to 80° by step scanning at 0.02° per step. The Rietveld refinement of the XRD pattern was performed by using the JANA2006 program. The pseudo-Voigt function was used to fit the diffraction peaks in the space group *Pbam*. The complex dielectric constant was measured in the temperature range T = 2–60 K with applied magnetic field H = 0–12 T at a frequency of 10 kHz by using a physical property measurement system (PPMS). For the dielectric measurements, the powder was pressed into a pellet of diameter 13 mm under the pressure of 30 kN by using the Paul-Otto Weber hydraulic press. The silver paste was used for forming a capacitor.

3. Results and discussion

The high quality single crystal of $\mathrm{NdMn_2O_5}$ is difficult to grow by using the flux method.[23,24] However, the polycrystalline $\mathrm{NdMn_2O_5}$ has been synthesized by the chemical transport method under high oxygen pressure.[25] Here, we report the successful synthesis of polycrystalline $\mathrm{NdMn_2O_5}$ by using the sol–gel method for the first time. Figure 1 presents the XRD pattern of polycrystalline $\mathrm{NdMn_2O_5}$ at room temperature. The XRD pattern is analyzed by using the Rietveld refinement technique assuming an orthorhombic structure with *Pbam* space group (see inset of Fig. 1). A good agrement has been found between the refined and the observed XRD patterns as all XRD peaks are fitted, which indicates the single phase formation of the material and no trace of any impurity. The obtained unit cell parameters are a = 7.51(3) Å, b = 8.62(2) Å, and c = 5.70(3) Å, which are consistent with the previously reported values.[12]

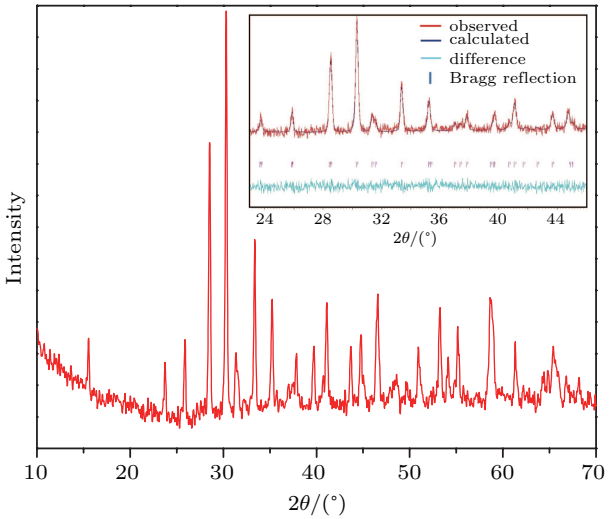


Fig. 1. (color online) Room temperature XRD pattern of polycrystalline $\mathrm{NdMn_2O_5}$. Inset shows the Rietveld refinement of the XRD curve by using the JANA2006 program. The calculated crystallographic data are R_P = 8.35, R_wp = 10.60, and GOF = 1.04.

The study of dielectric properties is an essential tool to identify the multiferroicity. Figure 2 shows the temperature variation of the dielectric constant during both heating and cooling with zero magnetic field. The dielectric constant increases sharply at $T_\mathrm{N} \sim 31$ K, which is referred to as the Néel temperature.[17,26] Just below T_N, there is a sharp peak indicating a small thermal effect as observed previously.[17,26] This sharp peak at $T_\mathrm{C} \sim 26$ K is attributed to the ferroelectric peak as observed in other $R\mathrm{Mn_2O_5}$.[27] It is worth mentioning that the thermal hysteresis of T_C indicates the first order phase transition similar to the other ferroelectric members. A slight change in the dielectric curve observed at $T_X \sim 16$ K may be associated with another weak dielectric anomaly.

If this anomalous behavior appeared as a sharp step, it might be attributed to excitation of electromagnons.[28,29] Here, we suggest that the anomaly at $T_X \sim 16$ K may not be related to any electromagnon excitation, rather it is related to a slight change in the magnetic propagation vector.[17,26] The most interesting finding is the observation of the low temperature anomaly at $T_\mathrm{Nd} \sim 4$ K, which is attributed to the independent Nd^{3+} magnetic ordering as observed in other $R\mathrm{Mn_2O_5}$ (R =Tb,[2] Gd,[20] Dy,[21] Er,[30] Tm,[31] and Yb[24]). Chattopadhyay *et al.* failed to observe the low temperature independent Nd^{3+} ordering in their dielectric measurements.[17,26] However, we have clearly observed Nd^{3+} ordering in our dielectric measurements, which is consistent with the magnetic susceptibility and neutron diffraction measurements on $\mathrm{NdMn_2O_5}$.[17,26]

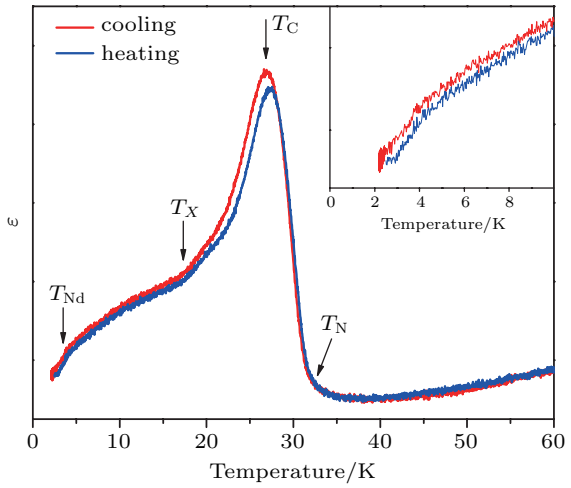


Fig. 2. (color online) Dielectric constant ε of $NdMn_2O_5$ at zero magnetic field. The arrows indicate the transition temperatures between different magnetic phases.

We have also measured the dielectric constant under a strong magnetic field in order to identify the magnetoelectric effect in $NdMn_2O_5$. Figure 3 demonstrates the variation in the dielectric constant under a magnetic field up to 12 T. Interestingly, the dielectric constant remains robust against the external magnetic field at the most prominent phase transitions (T_N, T_C, and T_X), however the anomaly at T_{Nd} smoothly vanishes with increasing magnetic field. The anomaly at T_{Nd} shows an interesting magnetoelectric behavior and is quite similar to that observed for other members of the RMn_2O_5 family.[20,21] Astonishingly, no magnetoelectric excitation is observed in the paramagnetic phase (above T_N) as observed in the case of $GdMn_2O_5$[20] and $DyMn_2O_5$[21] that gradually moves to higher temperature with increasing field. This reflects the role of the R^{3+} ions in the paramagnetic phase of RMn_2O_5, which is an unusual result and the origin of this discrepancy will be discussed later.

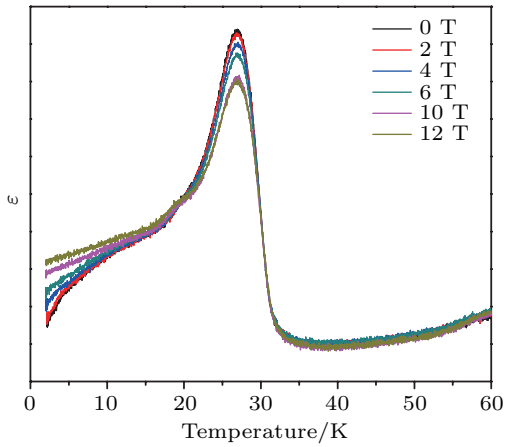


Fig. 3. (color online) Temperature dependent dielectric constant ε for $NdMn_2O_5$ at various magnetic fields up to 12 T.

3.1. Magnetoelectric phase diagram

In order to elucidate the magnetic field effect on $NdMn_2O_5$, we have constructed the magnetoelectric phase diagram, as shown in Fig. 4. The phase boundaries defined by T_N, T_C, and T_X in the phase diagram remain robust under the external magnetic field. These phase boundaries correspond to the phase transitions PM/PE $\rightarrow$ ICM1/PE at T_N, ICM1/PE $\rightarrow$ ICM1/FE at T_C, and ICM1/FE $\rightarrow$ ICM2/FE at T_X, respectively (we have used the conventions for different phases (i.e., ICM1, ICM2, PE, FE) from Ref. [17]). At the lowest temperatures ($T < 5$ K), an additional structure is seen due to an ordered state of the Nd^{3+} spins, which corresponds to another phase transition ICM2/FE $\rightarrow$ CM+ICM2/FE.

The phase diagram for $H = 0$ exhibits similar phase sequences as observed through neutron diffraction.[17] Therefore, we suggest that fundamental physics behind the different phases is the same as that in the $NdMn_2O_5$ phase diagram as described in Ref. [17]. Above 3 T, the CM+ICM2/FE phase becomes unstable and merges with ICM2/FE as the field increases up to 12 T. A possible explanation for this unstable phase may be a reorientation of the Nd^{3+} sublattice under the external magnetic field.

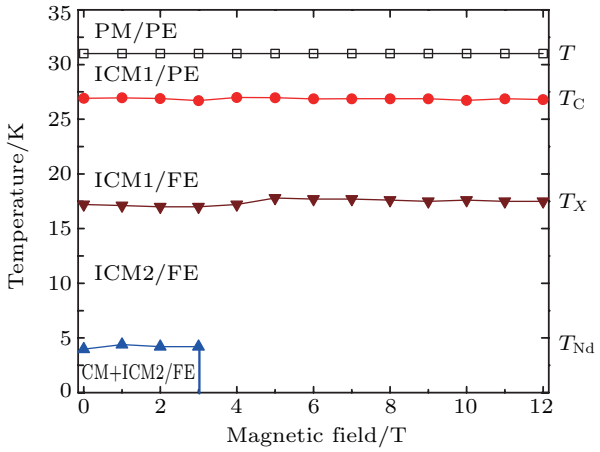


Fig. 4. (color online) Magnetoelectric phase diagram of $NdMn_2O_5$.

3.2. Discussion

The behavior of the dielectric constant is in line with the previous magnetic susceptibility and the neutron diffraction experiments on $NdMn_2O_5$.[17] The dielectric constant above 10 K is quite similar to the previously observed value and has shown no significant magnetoelectric effect. In most RMn_2O_5, the magnetoelectric effect appears in the low temperature phase due to different R^{3+} ions as observed here in the case of $NdMn_2O_5$. The magnetoelectric phase diagram clearly explains the magnetoelectric effect in the low temperature where the phase transition due to the Nd^{3+} sublattice smoothly vanishes with increasing field and merges with the well-defined ferroelectric phase. Further investigation on the field dependent polarization should be carried out in the low temperature phase.

Flores *et al.* have revealed the existence of phonon anomalies in the paramagnetic phase just above T_N for RMn_2O_5 (R = Bi, Eu, and Dy). They have found out that the phonon anomalies in the paramagnetic phase show strong dependencies with the ionic radii of the R^{3+} ions.[18] Thus it

reflects that the paramagnetic phase in $R\mathrm{Mn_2O_5}$ is also sensitive to the particular R^{3+} ions as well as the low temperature phase. However, no detailed investigation has yet been made in the paramagnetic phase of $R\mathrm{Mn_2O_5}$. Recently, we have clearly observed a sizeable change in the dielectric anomaly in the paramagnetic phase (45–65 K) with strong field dependencies in $\mathrm{GdMn_2O_5}$[20] and $\mathrm{DyMn_2O_5}$.[21] The absence of the dielectric anomaly in the paramagnetic phase (35–60 K) of $\mathrm{NdMn_2O_5}$ is worth noticing and may be related to the bigger ion $\mathrm{Nd^{3+}}$ (2.076 Å) as compared to $\mathrm{Gd^{3+}}$ (1.056 Å). Two possible scenarios arise due to different ionic radii of R^{3+}. First, the bigger ionic radius of $\mathrm{Nd^{3+}}$ shortening the bond length between adjacent $\mathrm{Mn^{4+}}$–$\mathrm{Mn^{4+}}$ spins through oxygen at the $\mathrm{Nd^{3+}}$ layer directly affects the k_z component of the propagation vector as described in Ref. [14]. This increases the J_1 exchange interaction, which differs appreciably from the one observed in $R\mathrm{Mn_2O_5}$ with small ionic radius. Secondly, there is also a sizable effect in the *ab* plane that increases the J_3 while it decreases the J_4 exchange interaction due to the bigger ionic radius of $\mathrm{Nd^{3+}}$.[14] We assume that R^{3+} plays a significant role even in the paramagnetic phase due to a different ionic radius that changes the bond length and thus affects the superexchange interactions.

Currently, we are unable to speculate further about this discrepancy that arises in the paramagnetic phase. A detailed investigation of neutron diffraction may help to explain the role of the R^{3+} ions in the paramagnetic phase. Also, a study of spin-phonon coupling in $\mathrm{NdMn_2O_5}$ through Raman and infrared active phonons with special emphasis in the paramagnetic phase would also be useful to confirm the role.

4. Conclusion

We have synthesized polycrystalline $\mathrm{NdMn_2O_5}$ and performed dielectric measurements under a strong magnetic field. Our results unveil an anomaly in the low temperature phase, attributed to the $\mathrm{Nd^{3+}}$ magnetic ordering. To summarize our results, a magnetoelectric phase diagram was constructed. We found that the main transitions defined by T_N, T_C, and T_X in the phase diagram remain robust under the external magnetic field. However, a strong magnetoelectric effect is observed for the transition at T_Nd that vanishes at fields higher than 3 T. Moreover, the absence of the dielectric anomaly in the paramagnetic phase may be due to the bigger ionic size of the $\mathrm{Nd^{3+}}$ ion, which directly influences the J_1 exchange interaction and results in a different magnetic correlation in the paramagnetic phase as compared to the small ionic radius of R^{3+} in the family of $R\mathrm{Mn_2O_5}$.

Acknowledgment

S. H. Bukhari acknowledges the financial support provided by the Higher Education Commission (HEC) of Pakistan through its IRSIP scholarship program (IRSIP 27 PS 28) and the Institute of Solid State Physics, Vienna University of Technology, Austria for providing research facilities.

References

[1] Higashiyama D, Miyasaka S and Tokura Y 2005 *Phys. Rev. B* **23** 064421
[2] Hur N, Park S, Sharma P A, Ahn J S, Guha S and Cheong S W 2004 *Nature* **429** 392
[3] Lee N, Vecchini C, Choi Y J, Chapon L C, Bombardi A, Radaelli P G and Cheong S W 2013 *Phys. Rev. Lett.* **110** 137203
[4] Fukunaga M, Sakamoto Y, Kimura H, Noda Y, Abe N, Taniguchi K, Arima T, Wakimoto S, Takeda M and Kakurai K 2009 *Phys. Rev. Lett.* **103** 077204
[5] Fukunaga M, Sakamoto Y, Kimura H and Noda Y 2011 *J. Phys. Soc. Jpn.* **80** 014705
[6] Ge H, Zhang X Q, Ke Y J, Jin J L, Liao Z X and Cheng Z H 2013 *Chin. Phys. B* **22** 057502
[7] Tang Z H, Tang M H, Lv X S, Cai H Q, Xiao Y G, Cheng C P, Zhou Y C and He J 2013 *J. App. Phys.* **113** 164106
[8] Tang Z, Wang B, Yang H, Xu X, Liu Y, Sun D, Xia L, Zhan Q, Chen B, Tang M, Zhou Y, Wang J and Li R 2014 *App. Phys. Lett.* **105** 103504
[9] Tang Z, Xiong Y, Tang M, Xiao Y, Zhang X, Yuan M, Ouyang J and Zhou Y 2014 *J. Mater. Chem. C* **2** 1427
[10] Kagomiya I, Kohn K and Uchiyama T 2002 *Ferroelectrics* **280** 131
[11] Alonso J, Casais M, Martínez-Lope M, Martinez J and Fernáandez-Díaz M 1997 *J. Phys.: Condens. Matter* **9** 8515
[12] Balédent V, Chattopadhyay S, Fertey P, Lepetit M, Greenblatt M, Wanklyn B, Saouma F, Jang J and Foury-Leylekian P 2015 *Phys. Rev. Lett.* **114** 117601
[13] Tachibana M, Akiyama K, Kawaji H and Atake T 2005 *Phys. Rev. B* **72** 224425
[14] Zobkalo I, Gavrilov S, Nyi N S, Barilo S and Shiryaev S 2014 *J. Magn. Magn. Mater.* **354** 85
[15] Blake G, Chapon L, Radaelli P, Park S, Hur N, Cheong S W and Rodriguez-Carvajal J 2005 *Phys. Rev. B* **71** 214402
[16] Doubrovsky C, André G, Gukasov A, Auban-Senzier P, Pasquier C, Elkaim E, Li M, Greenblatt M, Damay F and Foury-Leylekian P 2012 *Phys. Rev. B* **86** 174417
[17] Chattopadhyay S, Balédent V, Damay F, Gukasov A, Moshopoulou E, Auban-Senzier P, Pasquier C, André G, Porcher F and Elkaim E 2016 *Phys. Rev. B* **93** 104406
[18] García-Flores A F, Granado E, Martinho H, Urbano R R, Rettori C, Golovenchits E I, Sanina V A, Oseroff S B, Park S and Cheong S W 2006 *Phys. Rev. B* **73** 104411
[19] Cao J, Vergara L, Musfeldt J, Litvinchuk A, Wang Y, Park S and Cheong S W 2008 *Phys. Rev. B* **78** 064307
[20] Bukhari S H and Ahmad J 2016 *Physica B* **492** 39
[21] Bukhari S H and Ahmad J 2016 *Physica B* **503** 179
[22] Zhang X W, Lin T, Xu J, Xu L and Chen K J 2012 *Chin. Phys. B* **21** 018101
[23] Wanklyn B M 1972 *J. Mater. Sci.* **7** 813
[24] Koyata Y, Nakamura H, Iwata N, Inomata A and Kohn K 1996 *J. Phys. Soc. Jpn.* **65** 1383
[25] Euzen P, Leone P, Gueho C and Palvadeau P 1993 *Acta Crystallogr. C* **49** 1875
[26] Chattopadhyay S, Balédent V, Auban-Senzier P, Pasquier C, Doubrovsky C, Greenblatt M and Foury-Leylekian P 2015 *Physica B* **460** 214
[27] Hur N, Park S, Sharma P A, Guha S and Cheong S W 2004 *Phys. Rev. Lett.* **93** 107207
[28] Shuvaev A M, Travkin V D, Ivanov V Y, Mukhin A A and Pimenov A 2010 *Phys. Rev. Lett.* **104** 097202
[29] Sushkov A B, Aguilar R V, Park S, Cheong S W and Drew H D 2007 *Phys. Rev. Lett.* **98** 027202
[30] Kobayashi S, Osawa T, Kimura H, Noda Y, Kagomiya I and Kohn K 2004 *J. Phys. Soc. Jpn.* **73** 1031
[31] Kobayashi S, Kimura H, Noda Y and Kohn K 2005 *J. Phys. Soc. Jpn.* **74** 468